IJMS
Vol 47, No 4, July 2022

Original Article

Evaluation of Ultra-Low-Dose Chest Computed Tomography Images in Detecting Lung Lesions Related to COVID-19: A Prospective Study

Fariba Zarei[1], MD; Reza Jalli[1], MD; Sabyasachi Chatterjee[2], PhD; Rezvan Ravanfar Haghighi[1], PhD; Pooya Iranpour[1], MD; Vani Vardhan Chatterjee[3], PhD; Sedigheh Emadi[1], MSc

[1]Medical Imaging Research Center, Shiraz University of Medical Sciences, Shiraz, Iran;
[2]Ongil, 79 D3, Sivaya Nagar, Reddiyur Alagapuram, Salem, India;
[3]Department of Instrumentation and Applied Physics, Indian Institute of Science, Bangalore, India

Correspondence:
Rezvan Ravanfar Haghighi, PhD;
Medical Imaging Research Center, 8th Floor, Mohammad Rasool Allah Research Tower, Khalili St., Postal code: 71936-35899, Shiraz , Iran
Tel: +98 71 36281464
Fax: +98 71 36281506
Email: sravanfarr@gmail.com
Received: 06 May 2021
Revised: 23 July 2021
Accepted: 11 September 2021

Abstract

Background: The present study aimed to evaluate the effectiveness of ultra-low-dose (ULD) chest computed tomography (CT) in comparison with the routine dose (RD) CT images in detecting lung lesions related to COVID-19.

Methods: A prospective study was conducted during April-September 2020 at Shahid Faghihi Hospital affiliated with Shiraz University of Medical Sciences, Shiraz, Iran. In total, 273 volunteers with suspected COVID-19 participated in the study and successively underwent RD-CT and ULD-CT chest scans. Two expert radiologists qualitatively evaluated the images. Dose assessment was performed by determining volume CT dose index, dose length product, and size-specific dose estimate. Data analysis was performed using a ranking test and kappa coefficient (κ). $P<0.05$ was considered statistically significant.

Results: Lung lesions could be detected with both RD-CT and ULD-CT images in patients with suspected or confirmed COVID-19 ($\kappa=1.0$, $P=0.016$). The estimated effective dose for the RD-CT protocol was 22-fold higher than in the ULD-CT protocol. In the case of the ULD-CT protocol, sensitivity, specificity, accuracy, and positive predictive value for the detection of consolidation were 60%, 83%, 80%, and 20%, respectively. Comparably, in the case of RD-CT, these percentages for the detection of ground-glass opacity (GGO) were 62%, 66%, 66%, and 18%, respectively. Assuming the result of real-time polymerase chain reaction as true-positive, analysis of the receiver-operating characteristic curve for GGO detected using the ULD-CT protocol showed a maximum area under the curve of 0.78.

Conclusion: ULD-CT, with 94% dose reduction, can be an alternative to RD-CT to detect lung lesions for COVID-19 diagnosis and follow-up.

An earlier preliminary report of a similar work with a lower sample size was submitted to the arXive as a preprint. The preprint is cited as: https://arxiv.org/abs/2005.03347

Please cite this article as: Zarei F, Jalli R, Chatterjee S, Ravanfar Haghighi R, Iranpour P, Vardhan Chatterjee V, Emadi S. Evaluation of Ultra-Low-Dose Chest Computed Tomography Images in Detecting Lung Lesions Related to COVID-19:AProspectiveStudy.IranJMedSci.2022;47(4):338-349.doi:10.30476/IJMS.2021.90665.2165.

Keywords ● COVID-19 ● Radiation protection ● Computed tomography

What's Known

- Routine dose chest computed tomography (CT) can detect lung lesions related to COVID-19. However, it exposes patients to a high dose of ionizing radiation.
- The outcome of routine dose CT is comparable to the real-time polymerase chain reaction (RT-PCR) test.

What's New

- Ultra-low-dose chest CT, with 94% dose reduction, can detect lung lesions related to COVID-19 with acceptable image quality.

Introduction

Since the first reported cases of coronavirus disease 2019

(COVID-19) in December 2019, it has become a pandemic causing millions of deaths and continues to spread wildly through multiple mutations.[1] As a matter of public health policy and medical urgency, it is essential to develop a protocol for early detection, quick confirmation, and monitoring and prognosis of the disease through rapid testing. Some studies have proposed the application of unenhanced chest computed tomography (CT) to identify lung lesions related to COVID-19. This method can be considered a valuable diagnostic tool; however, its performance parameters should be compared with the real-time polymerase chain reaction (RT-PCR) test, which is currently the gold standard.[2, 3]

CT scans expose patients to a high dose of ionizing radiation, which in turn puts them at the risk of developing several stochastic effects including carcinomas.[4] However, our literature review has shown that chest X-rays can detect different types of lung lesions with less than 1 mSv effective dose (ED). This level of radiation is very close to the doses in both the posterior-anterior (PA) and lateral chest radiographs, when iterative reconstruction is used. This CT protocol is known as ultra-low-dose (ULD). It is shown that the ULD-CT chest image, due to its three-dimensional nature, allows detection of normal and abnormal structures better than the plain radiograph.[5-8] A recent study reported that a radiation dose of less than 1 mSv can be used to diagnose lung lesions related to COVID-19 in patients in the emergency department.[9]

In developing countries, such as Iran, lengthy laboratory tests such as RT-PCR are not readily accessible and often result in delays in medical interventions, the spread of infection, and increased patient load. As an alternative, a chest CT scan can play an important role in the early detection of lung lesions related to COVID-19. Given the low radiation dose, the ULD-CT protocol becomes more attractive, as it protects patients from excessive exposure to radiation.

Considering the rapid spread of COVID-19, several diagnostic methods are proposed, among which the CT scan has received recognition from medical experts.[10] Early detection of the disease is important. However, the RT-PCR test is quite time-consuming, and precious time may be lost before the actual treatment begins.[3] Furthermore, the RT-PCR test has a 30-60% sensitivity,[2] which is much lower than the CT chest scan.[11] While the usefulness of the RT-PCR test is not disputed, its limitations should be noted. In this context, the utility of chest CT scan as an early detection tool should be considered.[12]

Recently, the ULD chest CT scan has been used to detect pulmonary lesions, such as nodules in different types of lung diseases, for the diagnosis of lung cancer. In some studies, a few patients underwent both routine dose (RD) and ULD chest CT scans. The findings of these studies showed that images obtained from both CT protocols were of acceptable quality and showed the same anatomic details. The total radiation dose received by these patients was less than 6 mSv, which is lower than the proposed diagnostic reference level.[13-15]

As a consequence of the COVID-19 pandemic, there has been an increasing request for chest CT scans in 2020 than the previous years.[16] The present study aimed to evaluate the effectiveness of ULD-CT, using iterative modal reconstruction, to detect lung lesions not only for the diagnosis of COVID-19, but also for the follow-up. The findings of the study were justified based on experimental observations.

Materials and Methods

A prospective study was conducted during April-September 2020 at Shahid Faghihi Hospital affiliated with Shiraz University of Medical Sciences (Shiraz, Iran). The study was approved by the local Ethics Committee of the University (code: IR.SUMS.REC.1399.050).

A total of 273 volunteers (117 women and 156 men) aged 50±20 years with suspected COVID-19 (suffering from respiratory problems) participated in the study. The participants were selected primarily because they were referred to the hospital for a chest CT scan to determine the extent of lung infection. These individuals were requested to undergo an additional ULD-CT scan, free of charge. The participants were fully informed about the risks of exposure to an extra dose of radiation and written informed consent was obtained from each participant. The exclusion criteria were aged <18 years, patients with underlying diseases (e.g., cancer, cardiovascular disorders), severe respiratory distress, pregnancy, and those not signing the consent form.

The participants successively underwent RD-CT and ULD-CT chest scans, while blinded to the type of each scan. The scans were performed using a 128-MDCT system (Philips Healthcare Ingenuity, USA). In the case of the RD-CT protocol, a tube current of 120 kVp with 64<mAs<343 modulations was used to scan the chest, whereas ULD-CT scanning parameters were 80 kVp fixed at 25 mAs. Other scanning parameters common to both protocols were slice

thickness (2 mm and 5 mm), intervals, and gantry rotation time (0.4 sec). The RD-CT images (axial, sagittal, and coronal) were reconstructed using the iDose level 4 hybrid iterative reconstruction software (Philips Healthcare, USA). ULD-CT images were reconstructed using iterative modal reconstruction (IMR) level 1 (Philips Healthcare, USA). Dose indices such as volume CT dose index ($CTDI_{vol}$ measured in mGy) and dose length product (DLP measured in mGy×cm) were recorded using the picture archiving and communication system (PACS, INFINITT, South Korea). Size-specific dose estimate (SSDE) was determined using the effective cross-section of the patient on the image and the related conversion factor for 32 cm diameter polymethyl methacrylate (IBA Lifesciences, Germany) body phantom, as described by the American Association of Physics in Medicine (AAPM) report number 204.[17] This conversion factor was multiplied by the mean $CTDI_{vol}$ for each patient to calculate the SSDE. Effective dose (ED) was calculated by multiplying DLP with the conversion factor (mSv/mGy×cm).[18]

Qualitative Study

The chest CT images were displayed and evaluated using the MDMC-12133 diagnostic monitor (Barco NV, Belgium). The ULD-CT images were independently examined by two expert radiologists (each with over 10 years of experience), who were blinded to the reports of the RD-CT images and each other's activity. The results of ULD and RD chest CT scans were tabulated using Microsoft Excel (Microsoft Corporation, USA) and consolidated according to common features. The information included consolidation, nodules, atelectasis band (AT), ground-glass opacity (GGO), crazy-paving pattern, atoll sign, subpleural band; architectural distortion, vascular dilation, bronchiectasis, lymphadenopathy, lung cavitation; centrilobular nodule, mosaic attenuation; air trapping, air bronchogram, pleural effusion, pericardial effusion, emphysematous change, and gravity. Of these, only GGO, consolidation, atoll sign, and crazy-paving pattern are typical imaging features of COVID-19.[19] Quality assessment was performed by classifying the quality of images into uninterpretable, poor, acceptable, and good (scores of 1, 2, 3, and 4, respectively).

Quantitative Study

Signal-to-noise ratio (SNR) was measured for the air in the trachea and descending aorta on both the RD-CT and ULD-CT images. The mean±SD of the Hounsfield unit (HU) values for the region of interest (ROI) from the trachea and descending aorta, without contamination from the neighboring structures, were recorded. The measured SNR was used as a quantitative method for the evaluation of image quality and calculated according to the below formulas.[20-24]

$$Signal = 1 + HU_{mean}/1000 \quad \text{(i)}$$

$$Noise = \frac{SD\ of\ HU\ in\ ROI/\sqrt{n}}{1000} \quad \text{(ii)}$$

$$SNR = Signal/Noise \quad \text{(iii)}$$

where HU_{mean} and SD are the mean HU and standard deviation for each ROI. The number of pixels in ROI was calculated using the formula: $n=A_{ROI}/A_{pixel}$ (where A_{ROI} is the area of the ROI and A_{pixel} is the area of a single-pixel in mm^2). Note that $A_{pixel}=(FOV/512)^2$, where FOV denotes the field of view and the reconstruction matrix is 512×512.

Based on the definition of HU value,[25, 26] the mean value of the attenuation coefficient of a substance in the ROI is calculated:

$$\mu_{mean} = \mu_{water} \times signal \quad \text{(iv)}$$

Moreover, the fluctuation of the observed mean value is calculated as:

$$\sigma(\mu_{mean}) = \mu_{water} \times Noise \quad \text{(v)}$$

Statistical Analysis

The kappa coefficient (κ) was used to evaluate the inter-rater agreement between the expert radiologists, who examined the images. A κ value of 1 indicates full agreement between the opinions. A ranking test was used to determine the difference between the revealed image features from both the ULD-CT and RD-CT protocols. This test was only performed on the images of those participants, who tested positive for COVID-19 (n=29). The resulting U and the corresponding P values were calculated. The null hypothesis (H_0) was that the ULD-CT and RD-CT images are of comparable quality. The quantity "P" indicates the probability that H_0 can give a U value at least as extreme as given in the sample data. In accordance with common practice, the significance level was set at α=0.05. The hypothesis is rejected if P<α (i.e., if the probability of having a U greater than the observed value is less than 5%). We noted that for a sample size greater than eight, the distribution of the U value closely followed a normal distribution,[21] which made the calculation of the P value very simple. Therefore, the selected sample sizes (suspected COVID-19 cases: n=273, confirmed COVID-19 cases: n=29) were more than adequate and satisfied the above criteria.

For diagnostic purposes, parameters such as specificity, sensitivity, accuracy, and positive predictive value (PPV) were calculated

for COVID-19 related features, namely consolidation, GGO, crazy-paving pattern, and atoll sign. These parameters were calculated based on the presence of these features in the image, which was classified as true-positive (TP), true-negative (TN), false-positive (FP), and false-negative (FN). These parameters were calculated as:[27]

Sensitivity=TP/(TP+FN)
Specificity=TN/(TN+FP)
Accuracy=(TP+TN)/(TP+TN+FP+FN)
PPV=TP/(TP+FP)

In addition, the HU values for two features (consolidation and GGO) were noted for the RD-CT and ULD-CT images. A discrimination criterion was selected and the receiver-operating characteristic (ROC) curve was plotted using the PCR test results as a reference.

Results

Qualitative Evaluations

Both radiologists concluded that images obtained using the ULD-CT protocol (94% dose reduction) revealed all lung lesions related to COVID-19 similar to those detected with the RC-CT protocol. They also reported that the image quality of ULD-CT was acceptable compared to that of RD-CT. The agreement between the two radiologists was excellent (κ=1), indicating that both protocols could equally detect different types of lung lesions related to COVID-19 as well as other causes. Sample ULD-CT and RD-CT images from two COVID-19 patients are presented in figures 1 and 2.

Chest CT images in figures 1 (a-f) and 2 (a-d) are of COVID-19 patients. They were scanned

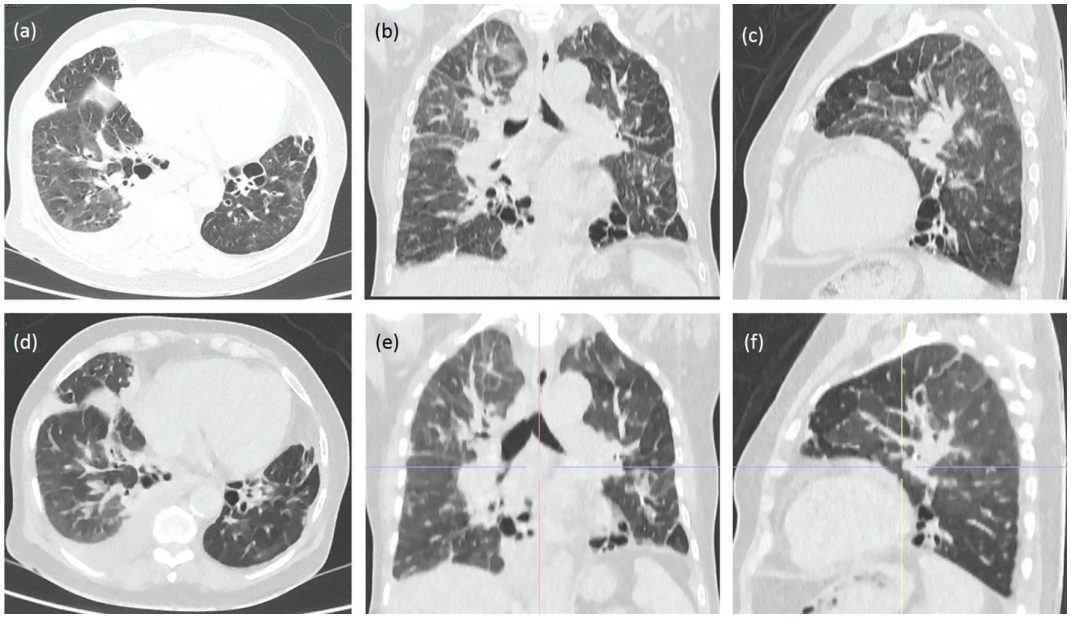

Figure 1: These figures show chest CT images of a 45-year-old female COVID-19 patient. Top row images show consolidation and crazy-paving pattern in (a) axial, (b) coronal, and (c) sagittal views using the RD-CT protocol. Bottom row images show the same features in (d) axial, (e) coronal, and (f) sagittal views using the ULD-CT protocol with 94% dose reduction.

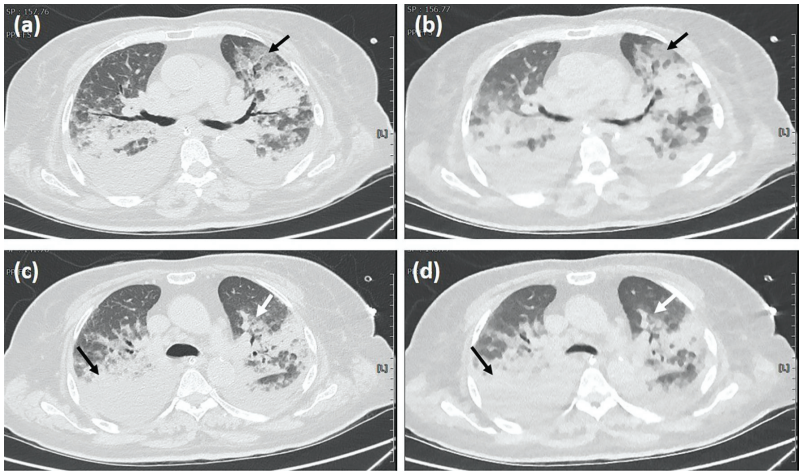

Figure 2: The axial chest CT images of a 71-year-old female COVID-19 patient are shown. Crazy-paving pattern (black arrow) is shown using the (a) RD-CT and (b) ULD-CT protocols. Ground-glass opacity (white arrow) and consolidation (black arrow) are shown using the (c) RD-CT and (d) ULD-CT protocols.

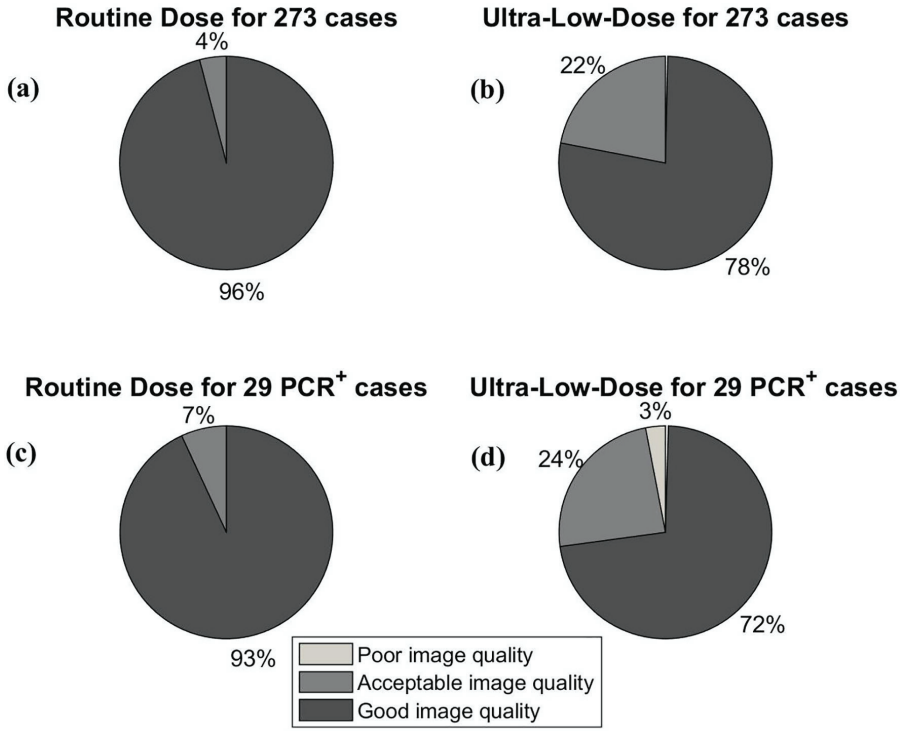

Figure 3: The image quality scores are compared between (a) RD-CT and (b) ULD-CT in 273 patients with suspected COVID-19. Image quality scores are also shown for (c) RD-CT and (d) ULD-CT in 29 confirmed COVID-19 patients (positive PCR).

Table 1: The image quality scores for routine dose and ultra-low-dose chest CT images in 29 patients with a positive PCR test

Patient number	Image quality score	
	Ultra-low-dose CT	Routine dose CT
1	Good	Good
2	Good	Good
3	Acceptable	Acceptable
4	Good	Good
5	Good	Good
6	Acceptable	Acceptable
7	Acceptable	Good
8	Acceptable	Good
9	Acceptable	Good
10	Good	Good
11	Good	Good
12	Poor	Good
13	Good	Good
14	Good	Good
15	Good	Good
16	Acceptable	Good
17	Good	Good
18	Good	Good
19	Good	Good
20	Good	Good
21	Good	Good
22	Good	Good
23	Good	Good
24	Good	Good
25	Acceptable	Good
26	Good	Good
27	Good	Good
28	Good	Good
29	Good	Good

using the RD-CT and ULD-CT protocols with an effective dose of 5±1.78 mSv and 0.25±0.05 mSv (about 94% dose reduction), respectively. Images with the 94% reduced dose also reveal crazy-paving pattern, GGO, atoll sign, and consolidation. The radiologists found the image quality just as satisfactory as the RD-CT chest images.

Qualitative Results

A comparison of image quality between the ULD-CT and RD-CT protocols in 273 patients with suspected COVID-19 is depicted as pie charts (figures 3a and 3b). The scores for the image quality of ULD-CT images were comparable to those of the RD-CT images. Similarly, image quality classifications for the 29 patients with confirmed COVID-19 are shown in figures 3c and 3d.

The image quality scores for ULD-CT and RD-CT images in 29 patients with confirmed COVID-19 are presented in table 1. The results showed that the image quality using the ULD-CT protocol was good, acceptable, and poor in 21 (72%), 7 (24%), and 1 (3%) of the patients, respectively, whereas, the quality using the RD-CT protocol was good and acceptable in 27 (93%) and 2 (7%) of the patients, respectively.

To assess the relative merits of RD-CT and ULD-CT images, a ranking test was performed using the image quality scores from all 273 patients. The results confirmed our hypothesis (P=0.160) that the data from both types of images had the same distribution (significance was set at α=0.05). The number of features detected from the RD-CT and ULD-CT images of patients with suspected (n=273) and confirmed (n=29) COVID-19 were comparable (table 2).

The most important features of COVID-19 were consolidation and GGO followed by atoll sign and crazy-paving pattern (table 2). The importance of detecting these features for the diagnosis of COVID-19 was evaluated in terms of specificity, sensitivity, accuracy, and PPV (table 3).

Based on the HU values of different cases, the results of qualitative evaluations showed that both the RD-CT and ULD-CT protocols had good efficacy and were effective in detecting lung lesions (table 4). Accordingly, discrimination criteria for consolidation and GGO were defined as:

- Consolidation: The HU value of the negative PCR cases is greater than or equal to the HU values of the positive cases.
- GGO: The HU value of the positive PCR cases is greater than the HU values of the negative cases.

Table 2: The number of features detected from the routine dose and ultra-low-dose CT images of patients with suspected or confirmed (positive PCR test) COVID-19

Feature	Patients with suspected COVID-19 (n=273)		Patients with confirmed COVID-19 (n=29)	
	Routine dose	Ultra-low-dose	Routine dose	Ultra-low-dose
Consolidation	54	59	15	17
Ground-glass opacity	69	101	18	18
Crazy paving	6	6	2	2
Atoll sign	6	6	4	4
Bronchiectasis	15	15	3	3
Plural effusion	52	52	6	6
Air bronchogram	13	13	3	3
Emphysematous change	25	25	0	0
Atelectasis band	20	20	1	1
Lymphadenopathy	7	6	0	0
Centrilobular nodule	9	9	1	1
Mosaic attenuation	23	22	2	0
Air trap	3	3	0	0

Table 3: The result of sensitivity, specificity, accuracy, and positive-predictive value calculations for the features consolidation, ground-glass opacity, crazy-paving pattern, and atoll sign

Feature	Sensitivity (%)		Specificity (%)		Accuracy (%)		PPV[$] (%)	
	RD[*]	ULD[#]	RD	ULD	RD	ULD	RD	ULD
Consolidation	52	60	84	83	81	80	28	29
Ground-glass opacity	62	62	79	66	77	66	26	18
Atoll sign	14	14	90	99	90	90	91	75
Crazy-paving pattern	7	7	98	98	87	89	50	33

[$]Positive predictive value; [*]Routine dose; [#]Ultra-low-dose

Table 4: The HU values for axial CT images of consolidation and ground-glass opacity in cases with positive and negative PCR tests using the routine dose and ultra-low-dose CT protocols

	Consolidation				Ground-glass opacity			
	Positive PCR		Negative PCR		Positive PCR		Negative PCR	
	RD*	ULD#	RD	ULD	RD	ULD	RD	ULD
Hounsfield unit (mean±SD)	20±15	16±23	29±60	26±10	-327±11	-288±11	-445±18	-439±15

*Routine dose; #Ultra-low-dose

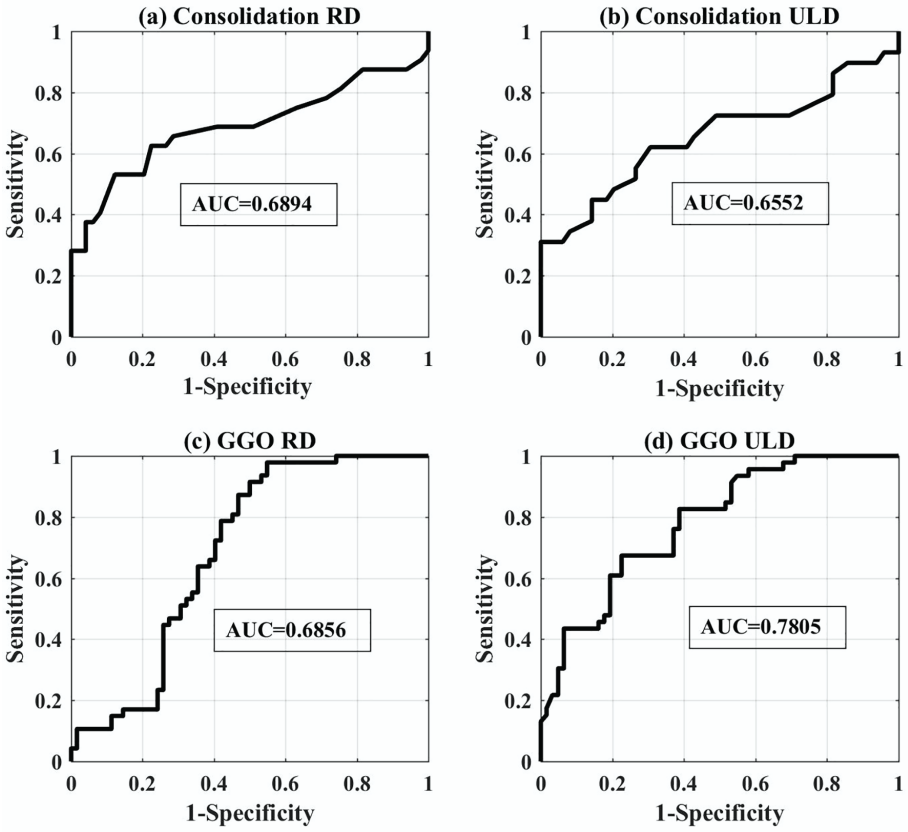

Figure 4: The ROC curve for consolidation and ground-glass opacity detected using the routine dose (a, c) and ultra-low-dose (b, d) CT protocols, respectively.

The efficacy of the above-mentioned discrimination criteria was analyzed using the ROC curve (figure 4) by comparing the area under the curve (AUC) for different cases.[22-24] Analysis of the ROC curves for consolidation and GGO detected with the RD-CT and ULD-CT showed a maximum AUC value of 0.78 for GGO on the ULD-CT image, whereas all others had an AUC<0.7 (figure 4). For GGO on the ULD-CT image, an optimal cut-off of HU>-243 can be used for patients, who test positive on RT-PCR, which corresponds to a sensitivity of 0.83 and 1-specificity of 0.40.

Quantitative Evaluations

HU values in the trachea and descending aorta were determined. On average, the ROI was 55 mm^2 containing 55 pixels. The results showed that these values were comparable in both protocols (table 5). Hence, grayscale levels and fluctuations on the images are also comparable. Since the HU_{mean} values obtained from each protocol were very close, we hypothesize that they have the same distribution. This hypothesis was verified using the *t* test for the aorta (P=0.276) and trachea (P=0.202); both >0.05.

The SNR and pixel noise were calculated for the HU_{mean} values of the air inside the trachea and descending aorta for both the ULD-CT and RD-CT images (formulas *i* and *ii*). These estimates revealed that the SNR for both images was comparable (table 6). However, the difference in SNR between the protocols requires further explanation. Based on the above-mentioned formulas (*i-v*), the mean HU value determines the mean attenuation coefficient of the substance for the ROI (iv). The fluctuations of the measured mean of HU are $\sigma[\mu_{mean}]$, as calculated using the formula (*ii*). Thus, based on the HU values (table 5), in the case of the trachea μ_{mean} for RD-CT and ULD-CT is equal to $0.025\times\mu_{water}$ and $0.028\times\mu_{water}$,

Table 5: HU values in the aorta and trachea for routine dose and ultra-low-dose CT protocols

Parameter	Protocol	Aorta	Trachea
Hounsfield unit (mean±SD)	Routine dose	46±37	-975±36
	Ultra-low-dose	49±39	-972±41

On average, the ROI was 55 mm^2 containing 55 pixels.

Table 6: Signal-to-noise ratio and pixel noise were measured in the descending aorta and trachea for axial chest CT images of patients with suspected COVID-19 using routine dose and ultra-low-dose CT protocols

Protocol	SNR*		Pixel noise	
	Aorta	Trachea	Aorta	Trachea
Routine-dose	360	6	37	36
Ultra-low-dose	316	4	39	41

*Signal-to-noise ratio; On average, the ROI was 55 mm^2 containing 55 pixels

respectively, with the corresponding $\sigma[\mu_{mean}]$ of $0.004\times\mu_{water}$ and $0.007\times\mu_{water}$. Thus, to observe the trachea, the SNR for RD-CT and ULD-CT are 6.25 and 4.0, respectively. While the trachea is largely an air-filled object, the aorta is a wide artery filled with blood. Therefore, for the case of the aorta, μ_{mean} for RD-CT and ULD-CT are $1.046\times\mu_{water}$ and $1.049\times\mu_{water}$, respectively, with the corresponding $\sigma[\mu_{mean}]$ of $0.0029\times\mu_{water}$ and $0.0033\times\mu_{water}$. Thus, the SNR for RD-CT and ULD-CT are 360 and 318, respectively.

Dose Assessment

The results of CT dose measurements showed that the $CTDI_{vol}$ of the ULD-CT protocol was fixed at 0.5 mGy and the mean DLP was 17 (15.6-20.2) mGy×cm. The mean of $CTDI_{vol}$ and DLP in RD-CT of patients with suspected COVID-19 was about 11 (6.6-20) mGy and 400 (255-700) mGy×cm, respectively. The SSDE for RD-CT and ULD-CT was 13±4 (5-29) mGy and 0.66±0.08 (0.51-0.89) mGy, respectively. This shows that the CT dose indicators (including $CTDI_{vol}$, DLP, and SSDE) of RD-CT and ULD-CT were significantly different. Estimated ED for the RD-CT protocol in patients with suspected or confirmed COVID-19 was 5.7 mSv, which is 22-fold higher than the ULD-CT protocol (ED: 0.246±0.055 mSv).

Discussion

The findings of the present study indicate that images obtained using the ULD-CT protocol have adequate quality and clarity for the diagnosis of COVID-19 infection. Based on radiological images, all COVID-19 features identified on the RD-CT images were also detectable by ULD-CT. The results of ROC analysis for consolidation and GGO showed that chest CT images are reliable for the overall diagnosis of COVID-19. We also demonstrated the reliability of ULD-CT images for this purpose, which was the primary objective of our study. The most interesting finding was the result of the ROC analysis of ULD-CT images that showed an AUC of 0.78 for GGO. However, further studies are required to substantiate this finding. The most appropriate cut-off for the identification of lung lesions related to COVID-19 is HU>-243, which corresponds to a sensitivity of 0.80 and 1-specificity of 0.40. The false-positive rate was slightly high which could be due to the limited sensitivity of the PCR test, although it is considered the gold standard.

Previous studies have reported high sensitivity (97%) of CT imaging for detecting GGO.[3, 10] However, our results showed a sensitivity of 62% for both the RD-CT and ULD-CT. Moreover, we determined the specificity of 79% and 66% for the RD-CT and ULD-CT, respectively, which is much higher than previously reported (25%). However, in line with previous studies,[3, 10] we determined the accuracy of 66% and 77% for the RD-CT and ULD-CT, respectively.

GGO develops at the onset of disease and is a classic early finding on CT scans, thus an important feature for the diagnosis of COVID-19.[28-30] However, as GGOs are non-uniform objects composed of air pockets and tiny particles, their X-ray attenuation coefficients would be low, generating diffuse CT images. To obtain improved CT images of these structures, it is necessary to enhance photoelectric absorption using low-energy photons. This is the process used in the ULD-CT in which X-ray photons of lower energy (i.e., higher attenuation coefficient) are used while cutting down the photon flux. For this reason, ULD-CT detects a higher number of GGOs than RD-CT (table 2). If confirmed, this phenomenon would be useful in early detection of COVID-19. However, since we compared our data with those of RT-PCR, which has only 30-60% sensitivity, the ULD-CT data included a high number of false-positive results and consequently lower specificity than the RD-CT. Further studies on this topic are recommended.

Other advantages of the ULD-CT are the attenuation of X-ray and lower SNR. Previous studies have shown that reducing tube voltage (kVp) increases image contrast.[31-33] This is logical, since lower tube voltages (kVp) emit more low-energy X-ray photons, which have perceptibly different photoelectric attenuations for substances with slightly different atomic numbers.[34, 35] This basic contrast enhancement is further improved using the iterative reconstruction that further reduces SNR.[36, 37]

The results showed that the data obtained from both protocols were extremely close to each other. This implies that for observing gray levels in the trachea, the difference in the mean gray levels between both protocols would be within 0.3%. Furthermore, the gray levels in both protocols can fluctuate within 0.3% of their respective mean values in the ROI. In short, since the SNR in both protocols was of the same order (360 and 316, within about 12% of each other), both offer the same level of noise reduction. This means that the performance of the ULD-CT is comparable to the RD-CT.

Concurrent with our study, Dangis and colleagues reported the use of a low-dose submillisievert chest CT for the diagnosis of COVID-19.[9] The main disadvantage of the submillisievert protocol is its rather higher mean ED (0.56 mSv) than that of the ULD-CT protocol (0.256 mSv). Besides, physical explanations for the attenuation coefficient proved that the structures observed in our images were not due to noise contamination. Overall, our proposed protocol offers the lowest radiation dose that has been reported so far. Moreover, the total radiation dose our participants were exposed to with both the RD-CT and ULD-CT was less than the proposed diagnostic reference level.[14]

With the aim of protecting patients from excessive exposure to radiation, the ULD-CT images were also assessed for their usefulness during follow-up. We found that these images provided an accurate and detailed image of the lung lesions comparable to the RD-CT. This is particularly important in the context of using CT scan images as a tool for the early detection of lung lesions in patients with suspected COVID-19. Considering the fact that the number of chest CT scans has drastically increased during the COVID-19 pandemic, CT dose optimization is crucial to reduce the risk of stochastic effects of radiation, genetic or carcinogenic, to a reasonable level, especially in pediatric, young, and pregnant patients.

In terms of image quality, we found that ULD-CT images at 80 kVp were of the same adequate quality as those obtained with RD-CT. This finding was in line with a previous study reporting that HU values and contrast-to-noise ratio of parenchymal organs and vessels gave better results at 80 kVp than at 120 kVp.[38] Overall, in terms of noise criteria, there is no significant difference between the two protocols. However, the appearance of the ULD-CT image is different from RD-CT due to a slightly higher noise level. Nonetheless, lung lesions can be distinguished using the ULD-CT protocol. Moreover, the presence of consolidation, GGO, atoll sign, and crazy-paving pattern, observed in the images of COVID-19 patients, shows that CT imaging modality is not only a viable diagnostic tool for the early identification of COVID-19, but also for the follow-up.

Conclusion

ULD chest CT (94% dose reduction) in conjunction with IMR level 1 can be used to detect lung lesions in patients with suspected COVID-19. These images can also be used during follow-up to prevent repeated exposure of patients to excessive doses of radiation and subsequent stochastic effects. Combating repeated waves of COVID-19 poses a major challenge, and non-invasive procedures are essential for rapid and effective diagnosis. ULD-CT imaging has the potential to meet this challenge.

Acknowledgment

The study was financially supported by Shiraz University of Medical Sciences, Shiraz, Iran (project number 99-01-48-22204). The authors would like to thank the staff, in particular Ms. Sakineh Rezaei, at the CT Department of Shahid Faghihi Hospital for their technical support. The feedback from reviewers to improve the technical content of the manuscript is greatly appreciated.

Authors' Contribution

F.Z, R.R.H, and S.E contributed to data acquisition. R.R.H and V.V.C contributed to the conception or design of the work. F.Z, R.J, S.C and PI contributed to interpretation. SC contributed to analysis. All Authors contributed to drafting and revising the manuscript critically for important intellectual content. All authors have read and approved the final manuscript and agree to be accountable for all aspects of the work in ensuring that questions related to the accuracy or integrity of any part of the work are appropriately investigated and resolved.

Conflict of Interest

Dr. Reza Jalli, as the Editorial Board Member, was not involved in any stage of handling this manuscript. A team of independent experts were formed by the Editorial Board to review the article without his knowledge.

References

1 Organization WH [Internet]. WHO Coronavirus (COVID-19) Dashboard. WHO Coronavirus (COVID-19) Dashboard With Vaccination Data. [cited 26 Sep 2021]. Available from: https://covid19.who.int/

2 Fang Y, Zhang H, Xie J, Lin M, Ying L, Pang P, et al. Sensitivity of Chest CT for COVID-19: Comparison to RT-PCR. Radiology. 2020;296:E115-E7. doi: 10.1148/radiol.2020200432. PubMed PMID: 32073353; PubMed Central PMCID: PMCPMC7233365.

3 Ai T, Yang Z, Hou H, Zhan C, Chen C, Lv W, et al. Correlation of Chest CT and RT-PCR Testing for Coronavirus Disease 2019 (COVID-19) in China: A Report of 1014 Cases. Radiology. 2020;296:E32-E40. doi: 10.1148/radiol.2020200642. PubMed PMID: 32101510; PubMed Central PMCID: PMCPMC7233399.

4 Smith-Bindman R, Lipson J, Marcus R, Kim KP, Mahesh M, Gould R, et al. Radiation dose associated with common computed tomography examinations and the associated lifetime attributable risk of cancer. Arch Intern Med. 2009;169:2078-86. doi: 10.1001/archinternmed.2009.427. PubMed PMID: 20008690; PubMed Central PMCID: PMCPMC4635397.

5 Paks M, Leong P, Einsiedel P, Irving LB, Steinfort DP, Pascoe DM. Ultralow dose CT for follow-up of solid pulmonary nodules: A pilot single-center study using Bland-Altman analysis. Medicine (Baltimore). 2018;97:e12019. doi: 10.1097/MD.0000000000012019. PubMed PMID: 30142849; PubMed Central PMCID: PMCPMC6112944.

6 Jin S, Zhang B, Zhang L, Li S, Li S, Li P. Lung nodules assessment in ultra-low-dose CT with iterative reconstruction compared to conventional dose CT. Quant Imaging Med Surg. 2018;8:480-90. doi: 10.21037/qims.2018.06.05. PubMed PMID: 30050782; PubMed Central PMCID: PMCPMC6037949.

7 Kroft LJM, van der Velden L, Giron IH, Roelofs JJH, de Roos A, Geleijns J. Added Value of Ultra-low-dose Computed Tomography, Dose Equivalent to Chest X-Ray Radiography, for Diagnosing Chest Pathology. J Thorac Imaging. 2019;34:179-86. doi: 10.1097/RTI.0000000000000404. PubMed PMID: 30870305; PubMed Central PMCID: PMCPMC6485307.

8 Kim Y, Kim YK, Lee BE, Lee SJ, Ryu YJ, Lee JH, et al. Ultra-Low-Dose CT of the Thorax Using Iterative Reconstruction: Evaluation of Image Quality and Radiation Dose Reduction. AJR Am J Roentgenol. 2015;204:1197-202. doi: 10.2214/AJR.14.13629. PubMed PMID: 26001228.

9 Dangis A, Gieraerts C, De Bruecker Y, Janssen L, Valgaeren H, Obbels D, et al. Accuracy and Reproducibility of Low-Dose Submillisievert Chest CT for the Diagnosis of COVID-19. Radiol Cardiothorac Imaging. 2020;2:e200196. doi: 10.1148/ryct.2020200196. PubMed PMID: 33778576; PubMed Central PMCID: PMCPMC7233439

10 Carotti M, Salaffi F, Sarzi-Puttini P, Agostini A, Borgheresi A, Minorati D, et al. Chest CT features of coronavirus disease 2019 (COVID-19) pneumonia: key points for radiologists. Radiol Med. 2020;125:636-46. doi: 10.1007/s11547-020-01237-4. PubMed PMID: 32500509; PubMed Central PMCID: PMCPMC7270744.

11 Fang Y, Zhang H, Xu Y, Xie J, Pang P, Ji W. CT Manifestations of Two Cases of 2019 Novel Coronavirus (2019-nCoV) Pneumonia. Radiology. 2020;295:208-9. doi: 10.1148/radiol.2020200280. PubMed PMID: 32031481; PubMed Central PMCID: PMCPMC7233358.

12 Xie X, Zhong Z, Zhao W, Zheng C, Wang F, Liu J. Chest CT for Typical Coronavirus Disease 2019 (COVID-19) Pneumonia: Relationship to Negative RT-PCR Testing. Radiology. 2020;296:E41-E5. doi: 10.1148/radiol.2020200343. PubMed PMID: 32049601; PubMed Central PMCID: PMCPMC7233363.

13 Jalli R, Zarei F, Chatterjee S, Ravanfar Haghighi R, Novshadi A, Iranpour P, et al. Evaluation of Ultra-Low-Dose Chest CT Images to Detect Lung Lesions. Middle East Journal of Cancer. 2021. doi: 10.30476/MEJC.2021.87355.1410.

14 Ludwig M, Chipon E, Cohen J, Reymond E, Medici M, Cole A, et al. Detection of pulmonary nodules: a clinical study protocol to compare ultra-low dose chest CT and standard low-dose CT using ASIR-V. BMJ Open. 2019;9:e025661. doi: 10.1136/bmjopen-2018-025661. PubMed PMID: 31420379; PubMed Central PMCID: PMCPMC6701577.

15 Messerli M, Kluckert T, Knitel M, Walti S, Desbiolles L, Rengier F, et al. Ultralow dose CT for pulmonary nodule detection with chest x-ray equivalent dose - a prospective

intra-individual comparative study. Eur Radiol. 2017;27:3290-9. doi: 10.1007/s00330-017-4739-6. PubMed PMID: 28093625.
16 Azadbakht J, Khoramian D, Lajevardi ZS, Elikaii F, Aflatoonian AH, Farhood B, et al. A review on chest CT scanning parameters implemented in COVID-19 patients: bringing low-dose CT protocols into play. Egyptian Journal of Radiology and Nuclear Medicine. 2021;52:1-10. doi: 10.1186/s43055-020-00400-1.8.
17 Brady SL, Kaufman RA. Investigation of American Association of Physicists in Medicine Report 204 size-specific dose estimates for pediatric CT implementation. Radiology. 2012;265:832-40. doi: 10.1148/radiol.12120131. PubMed PMID: 23093679.
18 Mettler FA, Jr., Huda W, Yoshizumi TT, Mahesh M. Effective doses in radiology and diagnostic nuclear medicine: a catalog. Radiology. 2008;248:254-63. doi: 10.1148/radiol.2481071451. PubMed PMID: 18566177.
19 Hefeda MM. CT chest findings in patients infected with COVID-19: review of literature. The Egyptian Journal of Radiology and Nuclear Medicine. 2020;51:239. doi: 10.1186/s43055-020-00355-3. PubMed PMID: PMC7691695.
20 Daniel WW. Biostatistics : basic concepts and methodology for the health sciences. 9th ed. New Jersey: John Wiley & Sons; 2010.
21 Johnson R, Miller I, Freund J. Miller & Freund's Probability and Statistics for Engineers. 8th ed. New York: Pearson; 2011.
22 Mohanty NC. Signal processing: signals, filtering, and detection. Van Nostrand Reinhold electrical/computer science and engineering series. New York: Springer; 1987.
23 Frieden R. Probability, statistical optics, and data testing: a problem solving approach. New York: Springer; 2001. p. 258–60 . doi: 10.1007/978-3-642-56699-8.
24 Helstrom CW. Statistical Theory of Signal Detection. 2nd Ed. New York: Springer; 1960.
25 Kalender WA. Computed tomography: fundamentals, system technology, image quality, applications. Erlangen: Wiley-VCH; 2005. 372 p.
26 Seeram E. Computed Tomography-E-Book: Physical Principles, Clinical Applications, and Quality Control. 2nd ed. Newberg: Saunders Company; 2001. 560 p.
27 Saha GB. Structure of Matter. In: Saha GB, editor. Physics and Radiobiology of Nuclear Medicine. New York: Springer; 2013. p. 1-10.
28 Wang D, Hu B, Hu C, Zhu F, Liu X, Zhang J, et al. Clinical Characteristics of 138 Hospitalized Patients With 2019 Novel Coronavirus-Infected Pneumonia in Wuhan, China. JAMA. 2020;323:1061-9. doi: 10.1001/jama.2020.1585. PubMed PMID: 32031570; PubMed Central PMCID: PMCPMC7042881.
29 Ye Z, Zhang Y, Wang Y, Huang Z, Song B. Chest CT manifestations of new coronavirus disease 2019 (COVID-19): a pictorial review. Eur Radiol. 2020;30:4381-9. doi: 10.1007/s00330-020-06801-0. PubMed PMID: 32193638; PubMed Central PMCID: PMCPMC7088323.
30 Liu M, Zeng W, Wen Y, Zheng Y, Lv F, Xiao K. COVID-19 pneumonia: CT findings of 122 patients and differentiation from influenza pneumonia. Eur Radiol. 2020;30:5463-9. doi: 10.1007/s00330-020-06928-0. PubMed PMID: 32399710; PubMed Central PMCID: PMCPMC7216854.
31 Dorneles CM, Pacini GS, Zanon M, Altmayer S, Watte G, Barros MC, et al. Ultra-low-dose chest computed tomography without anesthesia in the assessment of pediatric pulmonary diseases. J Pediatr (Rio J). 2020;96:92-9. doi: 10.1016/j.jped.2018.07.010. PubMed PMID: 30236593.
32 Khan AN, Khosa F, Shuaib W, Nasir K, Blankstein R, Clouse M. Effect of Tube Voltage (100 vs. 120 kVp) on Radiation Dose and Image Quality using Prospective Gating 320 Row Multi-detector Computed Tomography Angiography. J Clin Imaging Sci. 2013;3:62. doi: 10.4103/2156-7514.124092. PubMed PMID: 24605257; PubMed Central PMCID: PMCPMC3935263.
33 Seyal AR, Arslanoglu A, Abboud SF, Sahin A, Horowitz JM, Yaghmai V. CT of the Abdomen with Reduced Tube Voltage in Adults: A Practical Approach. Radiographics. 2015;35:1922-39. doi: 10.1148/rg.2015150048. PubMed PMID: 26473536.
34 Haghighi RR, Chatterjee S, Vyas A, Kumar P, Thulkar S. X-ray attenuation coefficient of mixtures: inputs for dual-energy CT. Med Phys. 2011;38:5270-9. doi: 10.1118/1.3626572. PubMed PMID: 21992344.
35 Haghighi RR, Chatterjee S, Tabin M, Sharma S, Jagia P, Ray R, et al. DECT evaluation of noncalcified coronary artery plaque. Med Phys. 2015;42:5945-54. doi: 10.1118/1.4929935. PubMed PMID: 26429269.
36 Park SB, Kim YS, Lee JB, Park HJ. Knowledge-based iterative model reconstruction (IMR) algorithm in ultralow-dose CT for evaluation of urolithiasis: evaluation of radiation dose reduction, image quality, and diagnostic performance. Abdom Imaging. 2015;40:3137-46. doi: 10.1007/s00261-015-0504-y. PubMed PMID: 26197735.
37 Wang Q, Geng H, Bai H, Wang R, Dong G.

Clinical Application of Iterative Reconstruction Technology in Ultra Low Dose Chest CT. Journal of Medical Imaging and Health Informatics. 2015;5:1599-602. doi: 10.1166/jmihi.2015.1617.

38 Nagayama Y, Tanoue S, Tsuji A, Urata J, Furusawa M, Oda S, et al. Application of 80-kVp scan and raw data-based iterative reconstruction for reduced iodine load abdominal-pelvic CT in patients at risk of contrast-induced nephropathy referred for oncological assessment: effects on radiation dose, image quality and renal function. Br J Radiol. 2018;91:20170632. doi: 10.1259/bjr.20170632. PubMed PMID: 29470108; PubMed Central PMCID: PMCPMC6190770.